

Bing Li · T.J. Nye · Don R. Metzger

## Multi-objective optimization of forming parameters for tube hydroforming process based on the Taguchi method

Received: 2 April 2004 / Accepted: 12 July 2004 / Published online: 13 April 2005  
© Springer-Verlag London Limited 2005

**Abstract** Tube hydroforming is an attractive manufacturing technology which is now widely used in many industries, especially the automobile industry. The purpose of this study is to develop a method to analyze the effects of the forming parameters on the quality of part formability and determine the optimal combination of the forming parameters for the process. The effects of the forming parameters on the tube hydroforming process are studied by finite element analysis and the Taguchi method. The Taguchi method is applied to design an orthogonal experimental array, and the virtual experiments are analyzed by the use of the finite element method (FEM). The predicted results are then analyzed by the use of the Taguchi method from which the effect of each parameter on the hydroformed tube is given. In this work, a free bulging tube hydroforming process is employed to find the optimal forming parameters combination for the highest bulge ratio and the lowest thinning ratio. A multi-objective optimization approach is proposed by simultaneously maximizing the bulge ratio and minimizing the thinning ratio. The optimization problem is solved by using a goal attainment method. An example is given to illustrate the practicality of this approach and ease of use by the designers and process engineers.

**Keywords** Finite element simulation · Goal attainment method · Multi-objective optimization · Taguchi method · Tube hydroforming

### 1 Introduction

Tube Hydroforming is a relatively new technology which has attracted the increasing attention of the automotive industry around the world. The goal of tube hydroforming is to form a straight or pre-bent tube into a die cavity of complex shape without any kind

of forming instability such as buckling, wrinkling, or bursting. In order to successfully obtain the final desired hydroformed parts, it is necessary to study the influence of the forming parameters on the hydroformability.

The influence of material properties and process parameters on the tube hydroforming process has been studied by means of experiments, analytical models, and finite element simulations. Carleer et al. [1] found that the anisotropy parameter and hardening exponent have a large impact on the shape of free expanded tubes, and the anisotropy parameter and friction coefficient have the biggest effect on strain distribution. Manabe and Amino [2] investigated the parameters influencing tube hydroforming by means of FEM simulations and experiments. They suggest that tubular material with a high hardening exponent and high anisotropy parameter should be selected, and good lubrication should be maintained to obtain the uniform wall thickness distribution. Boudeau et al. [3] used FEM to study the influence of material and process parameters on the necking and bursting. Ko and Altan [4] investigated the effects of the geometry parameters and process parameters in the tube hydroforming by a series of 2D FEM simulations. They found the internal pressure and the length of the tube have the greatest effects on the bulge of an axisymmetric part. Yang et al. [5] developed a numerical approach that can provide the sensitivity information of internal pressure and axial load on the tube hydroforming process. Consideration of the influence of the material, geometry, and process parameters simultaneously in one process has not been found in the literature.

The Taguchi method, an experimental design method, has been applied in a wide range of industries including the metal forming area [6–10]. The Taguchi method adopts a set of orthogonal arrays to analyze the effect of parameters on specific quality characteristics to determine the optimal combination of parameters. These kinds of arrays use a small number of experimental runs but get maximum information. In this study, we present a method to analyze the effects of the forming parameters on hydroformability by combining finite element analysis and the Taguchi method.

Problems related to the improvement of product quality and production efficiency can always be associated with the opti-

B. Li (✉) · T.J. Nye · D.R. Metzger  
Department of Mechanical Engineering,  
McMaster University,  
1280 Main Street West, Hamilton, ON, L8S 4L7, Canada  
E-mail: lib4@mcmaster.ca  
Fax: +1-905-5727944

mization procedures. The Taguchi method can optimize quality characteristics through the setting of design parameters, and can reduce the sensitivity of the system performance to sources of variation [11–15]. However, if more than one quality characteristic is simultaneously considered for the same process, the Taguchi method may not give a unique optimal combination of parameters, especially when these quality characteristics compete with each other. Attempting to optimize more than one objective makes the optimization problem a multi-objective one [16].

Mathematically, there are many methods to solve the multi-objective problem. Objectives usually conflict, so that the conditions leading to an optimal value of one objective give non-optimal values of the others. Under such circumstances, a *state* (i.e., a particular realization of problem parameter values) is preferred to another state if at least one objective is improved while none of the other objectives are worsened. If a state is found such that no other state is preferred in this way, it has the quality of being *Pareto optimal*. A given problem may have many states that are Pareto optimal, the collection of which form the *Pareto set*, or *Pareto front*, of the problem.

Common multi-objective solution methods are the weighted sum method, the  $\varepsilon$ -constraint method and the goal attainment method. The weighted sum method has a deficiency in that the Pareto optimal set is not available on non-convex portions in the criterion space. A difficulty of the  $\varepsilon$ -constraint method is to select a suitable  $\varepsilon$  to ensure a feasible solution, and a further disadvantage of this approach is that the use of hard constraints is rarely adequate for expressing true design objectives. The goal attainment method provides a convenient intuitive interpretation of the design problem which is solvable using standard optimization procedures, and there is always at least one Pareto optimal solution, also called the non-dominated solution, which balances the objectives in a unique and optimal way [17]. In this paper, a multi-objective optimization approach is proposed by integrating the classical mathematical optimization method with the Taguchi method, and the optimization problem is solved by the goal attainment method.

A free bulging tube hydroforming process is one of the most important processes for the research on tube hydroformability because it has many forming parameters involved in affecting its hydroformability. The objective of the free bulging process is to get a high bulge ratio while no necking failure happens. How to get an optimal combination of the forming parameters for satisfying these objectives is discussed in this paper, and a given free bulging tube hydroforming process is employed as an example to illustrate the proposed approach.

## 2 Methodology

The Taguchi method considers three stages in a process development: (1) system design, (2) parameter design, and (3) tolerance design. In system design, the engineer uses scientific and engineering principles to determine the basic configuration. In the parameter design stage the specific values for the system parameters are determined. Tolerance design is used to specify the best tolerances for the parameters [13]. Among these stages, parameter design is the key step in the Taguchi method to achieving high quality without increasing cost. To obtain high forming performance in the tube hydroforming process, the parameter design approach proposed by the Taguchi method is adopted in this paper.

The objective of this paper is to investigate the influence of forming parameters on hydroformability to improve the hydroformed tube quality. The basic steps for achieving the above target are shown in Fig. 1. First, the quality characteristics and the forming parameters are selected, and the appropriate orthogonal array is constructed. The finite element simulation is performed based on the arrangement of the orthogonal array, and the results are then transformed into the Taguchi signal-to-noise (S/N) ratios. Statistical analysis of variance (ANOVA) is performed to see which parameters are significant. After eliminating the insignificant parameters, these steps are repeated with the remaining significant parameters to obtain more information of their effects on the quality characteristics. Empirical models are then built through regression of the significant parameters, and the multi-criteria optimization is performed to maximize these

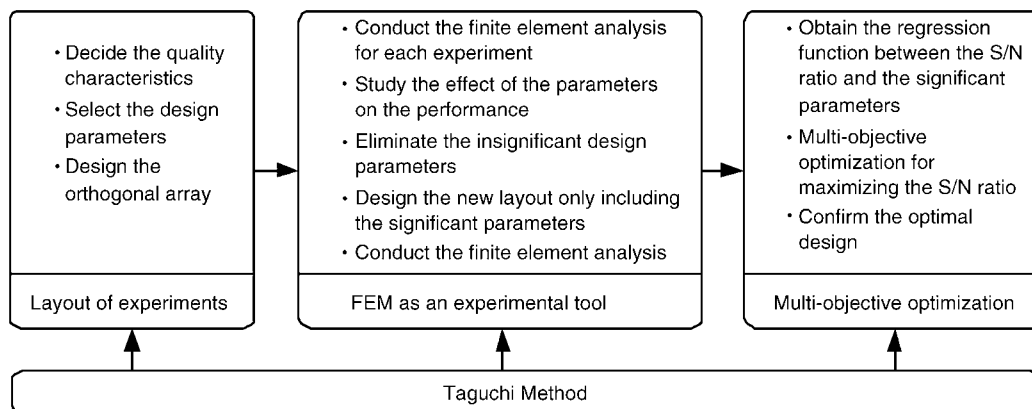


Fig. 1. Multi-objective optimization for tube hydroforming process using Taguchi method

S/N ratios. Finally, a confirmation experiment is conducted to verify the optimal parameter levels that are selected.

### 3 Free bulging tube hydroforming process

#### 3.1 FEM simulation

Finite element simulation is used as a numerical experimental tool in this study. Figure 2 shows the hydroforming process of free bulging of a straight tube with simultaneously applied internal pressure and axial force. The tooling was modeled as a rigid body, and the tube material was assumed to be isotropic elastic-plastic obeying the Ludwik–Hollomon hardening relationship  $\sigma = k\varepsilon^n$ . During simulation of the forming, the loading path strategy described in [2] was used. In this strategy, the internal pressure is applied independently and the axial load is applied according to the nominal stress ratio  $m$ . Table 1 shows the nominal values of the process parameters, geometries of the tube and tooling, and the material properties of the tubular blank for the finite element simulation. The explicit FEM code H3DMAP [18] was used for the analysis of the tube hydroforming process of free bulging.

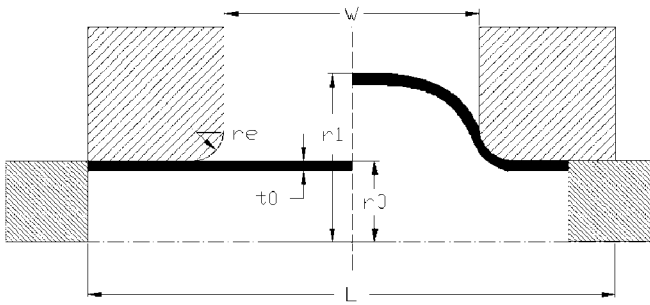


Fig. 2. Schematic view of free bulging tube hydroforming

Table 1. Parameters used in the FEM simulation

Material parameters	Value
Density $\rho$ (kg/m <sup>3</sup> )	7850
Young's modulus $E$ (GPa)	205
Hardening coefficient $K$ (MPa)	537
Hardening exponent $n$	0.227
Poisson's ratio $\nu$	0.3
Yield strength $\sigma_y$ (MPa)	240
Ultimate tensile strength $\sigma_u$ (MPa)	350
Geometry parameters	
Length of tube $L_0$ (mm)	200
Outer radius of tube $r_0$ (mm)	30
Thickness of tube $t_0$ (mm)	1.5
Die entry radius $r_e$ (mm)	10
Bulge width $W$ (mm)	100
Process parameters	
Internal pressure $P_f$ (MPa)	40
Nominal stress ratio $m$	0.4
Friction coefficient $\mu$	0.06

#### 3.2 Decision of quality characteristics and objective function

In the free bulging tube hydroforming process, the primary objective is to get the bulge ratio as high as possible without any failure happening. Among the three main failure modes involved in tube hydroforming, bursting failure is irrevocable while other failure modes like buckling and wrinkling are recoverable. Bursting is a consequence of necking, which causes fracture eventually. Although there are many different proposed criteria for predicting fracture in metal forming processes, there is no clearly preferred approach. Therefore, the commonly used thinning ratio criteria is used here as a measure of forming quality.

The thinning ratio as well as the bulge ratio is selected as the quality characteristics. The thinning ratio is defined by

$$\text{Thinning ratio}(\%) = \frac{t_0 - t_1}{t_0} \times 100 \quad (1)$$

where  $t_0$  is the original thickness of the tube as shown in Fig. 2 and  $t_1$  is the critical thickness of the hydroformed tube. The bulge ratios is defined by

$$\text{Bulge ratio}(\%) = \frac{r_1}{r_0} \times 100 \quad (2)$$

where  $r_1$  is the maximum radius of the hydroformed tube and  $r_0$  is the original radius of the tube as shown in Fig. 2. Two objective functions are chosen for this process. One is to obtain the minimum value of the thinning ratio, and the other is to obtain the maximum value of the bulge ratio.

#### 3.3 Selection of the parameters and construction of orthogonal array

Generally, there are three categories of parameters influencing hydroformability, i.e., geometry parameters, material parameters, and process parameters (Table 1). The eight forming parameters to be evaluated in this study are shown in Table 2. To evaluate these factors, three levels are chosen for each. For eight factors with three levels for each, the experimental layout of an  $L_{18}$  orthogonal array is selected for present research according to Taguchi's suggestion. Table 3 shows the  $L_{18}$  orthogonal array in which the 18 runs are carried out to investigate the effects of the eight factors.

Table 2. Level of forming parameters

Designation	Forming parameters	Level 1	Level 2	Level 3
A	Length of the tube (mm)	180	200	220
B	Thickness of tube (mm)	1.35	1.5	1.65
C	Die entry radius (mm)	8	10	12
D	Bulge width (mm)	90	100	110
E	Hardening exponent	0.207	0.227	0.247
F	Internal pressure (MPa)	36	40	44
G	Nominal stress ratio	0.2	0.4	0.6
H	Friction coefficient	0.02	0.06	0.1

**Table 3.** Taguchi's  $L_{18}$  orthogonal array

Run no.	Forming parameters							
	A	B	C	D	E	F	G	H
1	1	1	1	1	1	1	1	1
2	1	1	2	2	2	2	2	2
3	1	1	3	3	3	3	3	3
4	1	2	1	1	2	2	3	3
5	1	2	2	2	3	3	1	1
6	1	2	3	3	1	1	2	2
7	1	3	1	2	1	3	2	3
8	1	3	2	3	2	1	3	1
9	1	3	3	1	3	2	1	2
10	2	1	1	3	3	2	2	1
11	2	1	2	1	1	3	3	2
12	2	1	3	2	2	1	1	3
13	2	2	1	2	3	1	3	2
14	2	2	2	3	1	2	1	3
15	2	2	3	1	2	3	1	3
16	2	3	1	3	2	3	2	1
17	2	3	2	1	3	1	2	3
18	2	3	3	2	1	2	3	1

## 4 Results and discussion

### 4.1 Effects of forming parameters on the hydroformability

Two different quality characteristics are analyzed by using the S/N and ANOVA analyses based on the results of the FEM simulation corresponding to the above orthogonal array.

#### 4.1.1 S/N analyses

In the Taguchi method, the signal-to-noise (S/N) ratio is used to measure the quality characteristic deviating from the desired value. The S/N ratio is defined by

$$S/N = -10 \log(MSD) \quad (3)$$

where  $MSD$  is the mean square deviation for the quality characteristic.

Usually, there are three categories of quality characteristic in the analysis of the S/N ratio, i.e., the-lower-the-better, the-higher-the-better, and the-nominal-the-better. Thinning ratio in this study is the quality characteristic with the objective "the-lower-the-better". The mean square deviation for the-lower-the-better quality characteristic is given by

$$MSD = \frac{1}{n} \sum_{i=1}^n y_i^2 \quad (4)$$

where  $y_i$  is the value of the-lower-the-better quality characteristic and  $n$  is the number of the tests for a trial condition.

Bulge ratio is a quality characteristic with the objective "the-higher-the-better". The mean square deviation for the-higher-the-better quality characteristic is given by

$$MSD = \frac{1}{n} \sum_{i=1}^n \frac{1}{y_i^2} \quad (5)$$

where  $y_i$  is the value of the-higher-the-better quality characteristic. In the event the-nominal-the-better quality characteristic is desired, the mean square deviation would be

$$MSD = \frac{1}{n} \sum_{i=1}^n (y_i - S)^2 \quad (6)$$

where  $y_i$  is the value of the-nominal-the-better quality characteristic and  $S$  is the target value. Regardless of the category of the quality characteristic, a greater S/N ratio corresponds to better quality characteristics.

After conducting the FEM simulations and applying S/N analyses, the results of the bulge ratio and its S/N ratio in the 18 trial conditions are shown in Table 4. The average S/N ratio of the bulge ratio for each parameter at levels 1 to 3 are shown in Table 5 and plotted in Fig. 3. Table 6 shows the FEM results of the thinning ratio and its S/N ratio in the 18 trial conditions. The average S/N ratio of the thinning ratio for each parameter at levels 1 to 3 are shown in Table 7 and plotted in Fig. 4.

#### 4.1.2 ANOVA analyses

In order to investigate the effects of the forming parameters quantitatively, analysis of variance (ANOVA) is carried out.

**Table 4.** Bulge ratio values and its S/N ratio

Run no.	Bulge ratio	S/N ratio
1	1.448	3.215
2	1.982	5.942
3	1.923	5.679
4	1.596	4.060
5	2.029	6.145
6	1.449	3.221
7	1.691	4.564
8	1.439	3.162
9	1.590	4.030
10	1.678	4.498
11	1.719	4.704
12	1.640	4.297
13	1.498	3.510
14	1.639	4.293
15	1.853	5.358
16	1.744	4.828
17	1.492	3.473
18	1.597	4.065

**Table 5.** Average S/N ratio of the bulge ratio for each parameter

Designation	Forming parameters	Average S/N ratio		
		Level 1	Level 2	Level 3
A	Length of the tube	4.446	4.336	
B	Thickness of tube	4.723	4.431	4.020
C	Die entry radius	4.113	4.620	4.442
D	Bulge width	4.140	4.754	4.280
E	Hardening exponent	4.010	4.608	4.556
F	Internal pressure	3.480	4.481	5.213
G	Nominal stress ratio	4.556	4.421	4.197
H	Friction coefficient	4.319	3.568	5.287

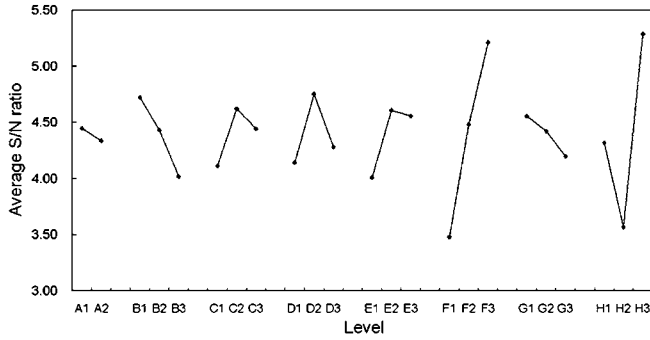


Fig. 3. Average effect diagram of forming parameter on the bulge ratio

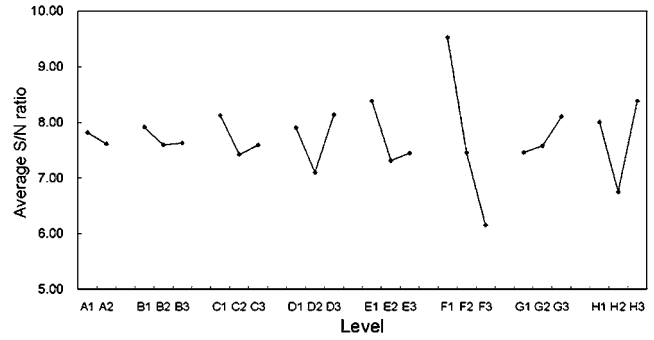


Fig. 4. Average effect diagram of forming parameter on the thinning ratio

Table 6. Thinning ratio values and S/N ratio

Run no.	Thinning ratio	S/N ratio
1	0.284	10.934
2	0.497	6.067
3	0.477	6.436
4	0.407	7.815
5	0.559	5.047
6	0.304	10.343
7	0.483	6.315
8	0.315	10.025
9	0.429	7.358
10	0.386	8.268
11	0.423	7.480
12	0.385	8.298
13	0.345	9.252
14	0.417	7.604
15	0.530	5.514
16	0.493	6.149
17	0.384	8.313
18	0.416	7.618

Table 7. Average S/N ratio of the thinning ratio for each parameter

Designation	Forming parameters	Average S/N ratio		
		Level 1	Level 2	Level 3
A	Length of the tube	7.815	7.611	
B	Thickness of tube	7.914	7.596	7.630
C	Die entry radius	8.122	7.423	7.594
D	Bulge width	7.902	7.100	8.137
E	Hardening exponent	8.382	7.311	7.446
F	Internal pressure	9.527	7.455	6.157
G	Nominal stress ratio	7.459	7.576	8.104
H	Friction coefficient	8.007	6.750	8.383

ANOVA tests for significant differences between the parameters by comparing variances. It uses the sum of squares to partition the overall variation from the average S/N ratio into the contribution by each of the parameters and the error.

The overall average S/N ratio is expressed as

$$\overline{S/N} = \frac{1}{k} \sum_{i=1}^k (S/N)_i \tag{7}$$

where  $k$  is the number of tests in the orthogonal array and  $(S/N)_i$  is the S/N ratio of the  $i$ th test. The sum of the squares due to the variation from the overall average S/N ratio is

$$SS = \sum_{i=1}^k ((S/N)_i - \overline{S/N})^2 \tag{8}$$

The sum of the squares due to the variation from the average S/N ratio for the  $i$ th factor is

$$SS_i = \sum_{j=1}^l T_j \times ((\overline{S/N})_{ij} - \overline{S/N})^2 \tag{9}$$

where  $l$  is the number of the factor levels ( $l = 3$  in this study),  $T_j$  is the number of the tests of the  $i$ th factor at the  $j$ th level, and  $(\overline{S/N})_{ij}$  is the average S/N ratio of the quality characteristic for the  $i$ th factor at the  $j$ th level. The percentage contribution of the  $i$ th factor is given by

$$P_i(\%) = \frac{SS_i}{SS} \times 100. \tag{10}$$

The results of ANOVA for the bulge ratio and thinning ratio are shown in Tables 8 and 9. From Table 8, it can be seen that the significant parameters influencing the bulge ratio are internal pressure and friction coefficient. The effect of length, thickness, die entry radius, bulge width, hardening exponent, and nominal

Table 8. Analysis of variance for bulge ratio

Parameters	Degree of freedom	Sum of squares	Contribution (%)
Length of the tube	1	0.055	0.37
Thickness of tube	2	0.747	5.10
Die entry radius	2	0.398	2.71
Bulge width	2	0.621	4.24
Hardening exponent	2	0.658	4.49
Internal pressure	2	4.543	31.00
Nominal stress ratio	2	0.198	1.35
Friction coefficient	2	4.458	30.42
Error	2	2.978	
Total	17	14.654	

stress ratio are very small compared to that of internal pressure and friction coefficient. These results are in good agreement with the results reported in the literature [2, 4, 19]. Table 9 shows the internal pressure is the most significant forming parameter affecting the thinning ratio, and the friction coefficient is the next most significant parameter.

The forming parameters except internal pressure and friction coefficient do not contribute much to the hydroformability, so they are eliminated from the optimization of the tube hydroforming process as discussed in the next section.

#### 4.2 Multi-objective optimization of tube hydroforming process

After eliminating the insignificant forming parameters, the analyses of the S/N ratio are conducted again with only the significant parameters, i.e., internal pressure and friction coefficient.

The same three levels of the internal pressure and friction coefficient as shown in Table 2 are chosen. A Taguchi  $L_9$  orthogonal array is selected for two factors with three levels, as shown in Table 10. Comparing Tables 3 and 10, shows the  $L_{18}$  orthogonal array used earlier is a fractional factorial array, while the  $L_9$  orthogonal array is a full factorial array in which all of the possible combinations of factor levels are tested. The last two columns in Table 10 represent the interaction of the two factors. Table 11 shows the FEM results of the bulge ratio and its S/N ratio in the nine trial conditions, and Table 12 shows the FEM results of the thinning ratio and S/N ratio. These tables

**Table 9.** Analysis of variance for thinning ratio

Parameters	Degree of freedom	Sum of squares	Contribution (%)
Length of the tube	1	0.188	0.40
Thickness of tube	2	0.183	0.39
Die entry radius	2	0.797	1.70
Bulge width	2	1.777	3.79
Hardening exponent	2	2.042	4.35
Internal pressure	2	17.341	36.97
Nominal stress ratio	2	0.709	1.51
Friction coefficient	2	4.387	9.35
Error	2	19.482	
Total	17	46.907	

**Table 10.** Taguchi's  $L_9$  orthogonal array

Run no.	Internal pressure ( $A'$ )	Friction coefficient ( $B'$ )	$A' \times B'$	$A' \times B'$
1	1	1	1	1
2	1	2	2	2
3	1	3	3	3
4	2	1	2	3
5	2	2	3	1
6	2	3	1	2
7	3	1	3	2
8	3	2	1	3
9	3	3	2	1

**Table 11.** Bulge ratio and S/N ratio

Run no.	Internal pressure (MPa) ( $A'$ )	Friction coefficient ( $B'$ )	$A' \times B'$	Bulge ratio	S/N ratio
1	36	0.02	0.720	1.412	2.999
2	36	0.06	2.160	1.419	3.038
3	36	0.1	3.600	1.424	3.070
4	40	0.02	0.800	1.591	4.036
5	40	0.06	2.400	1.603	4.100
6	40	0.1	4.000	1.638	4.286
7	44	0.02	0.880	1.767	4.945
8	44	0.06	2.640	1.787	5.043
9	44	0.1	4.400	1.831	5.255

**Table 12.** Thinning ratio and its S/N ratio

Run no.	Internal pressure (MPa) ( $A'$ )	Friction coefficient ( $B'$ )	$A' \times B'$	Thinning ratio	S/N ratio
1	36	0.02	0.720	0.293	10.653
2	36	0.06	2.160	0.303	10.381
3	36	0.1	3.600	0.311	10.135
4	40	0.02	0.800	0.399	7.973
5	40	0.06	2.400	0.411	7.730
6	40	0.1	4.000	0.433	7.264
7	44	0.02	0.880	0.479	6.399
8	44	0.06	2.640	0.493	6.137
9	44	0.1	4.400	0.516	5.747

show that increased internal pressure and increased friction coefficient each give higher bulge ratios, along with higher thinning ratios.

As mentioned earlier, the objectives of this study are to minimize the thinning ratio and maximize the bulge ratio. These two objectives conflict in the free bulge process since higher bulge ratios are highly correlated with higher thinning ratios, and vice versa. However, the use of the Taguchi S/N ratio assists in discriminating better quality characteristics, so the objectives in this study can be converted to simultaneously maximize the S/N ratio of the bulge ratio and thinning ratio.

Regression analyses are performed on the data in Tables 11 and 12 to get the relationship of the S/N ratios of the bulge ratio and thinning ratio with the forming parameters. The regression equations of the S/N ratio of the bulge ratio ( $(S/N)_{BR}$ ) and the S/N ratio of the thinning ratio ( $(S/N)_{TR}$ ) are given in Eqs. 11 and 12.

$$(S/N)_{BR} = -5.4 + 0.23A' - 12.31B' + 0.37A'B' \quad (11)$$

$$(S/N)_{TR} = 29.49 - 0.52A' + 0.55B' - 0.21A'B' \quad (12)$$

Although enough degrees of freedom are available in the data to estimate the main second order effect terms (i.e.,  $A^2$ ,  $B^2$ ), the coefficients of these terms are found to be not statistically significantly different from zero. The objective function for the

optimization can now be formulated as follows:

$$\begin{aligned} \text{Max :} & \quad \begin{bmatrix} (S/N)_{BR} \\ (S/N)_{TR} \end{bmatrix} \\ \text{Subject to :} & \quad 36 \leq \text{Internal pressure} \leq 44 \\ & \quad 0.02 \leq \text{friction coefficient} \leq 0.1 \end{aligned} \quad (13)$$

The solution to the above objective function will lead to a combination of minimum thinning ratio together with a maximum bulge ratio that is Pareto optimal.

The goal attainment method [20] is used to solve the above multi-objective optimization problem. Applying the method to Eq. 13 transforms it to the following formulation.

$$\begin{aligned} \text{Min :} & \quad \gamma \\ \text{Subject to :} & \quad (S/N)_{BR} - w_1\gamma \leq (S/N)_{BR}^{\ominus} \\ & \quad (S/N)_{TR} - w_2\gamma \leq (S/N)_{TR}^{\ominus} \\ & \quad 36 \leq \text{Internal pressure} \leq 44 \\ & \quad 0.02 \leq \text{friction coefficient} \leq 0.1 \end{aligned} \quad (14)$$

where  $\gamma$  is an unrestricted scalar,  $(S/N)_{BR}^{\ominus}$  is the maximum S/N ratio of the bulge ratio in Table 11,  $(S/N)_{TR}^{\ominus}$  is the maximum S/N ratio of the thinning ratio in Table 12,  $[(S/N)_{BR}^{\ominus}, (S/N)_{TR}^{\ominus}]$  is the goal of the set of objectives  $[(S/N)_{BR}, (S/N)_{TR}]$ , and the weighting vector  $[w_1, w_2]$  controls the relative degree of under- or overachievement of the goals. In this paper, the weighting vector  $w$  is made equal to the goal, so that the same percentage under- or overattainment of the goals is achieved [20]. The solution of Eq. 14 gives the optimal combination of internal pressure and friction coefficient, as shown in Table 13, along with the estimated S/N ratios of bulge ratio  $(S/N)_{BR}^*$  and thinning ratio  $(S/N)_{TR}^*$ . From the Tables 11-13, it can be seen that this Pareto optimal combination of the forming parameters comes as a trade-off between the two objectives.

### 4.3 Confirmation experiments

Confirmation is carried out at the optimum setting of the significant forming parameters while keeping the remaining parameters as the nominal values. The obtained bulge ratio is 1.596 and its S/N ratio is 4.061, the obtained thinning ratio is 0.391 and its S/N ratio is 8.156. Comparing with the results obtained in the nominal case using data in Table 1, i.e., the bulge ratio is 1.580 and the thinning ratio is 0.393, it shows that both the bulge ratio and thinning ratio are improved by using the optimal setting of

**Table 13.** Optimal combination of parameters and estimated S/N ratio

Internal pressure (MPa)	Friction coefficient (C)	$(S/N)_{BR}^*$	$(S/N)_{TR}^*$
40.73	0.02	4.023	8.150

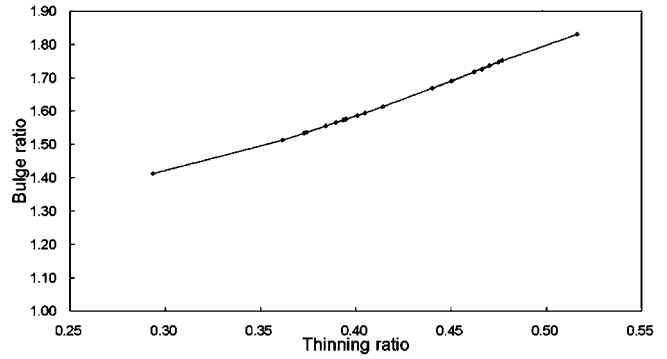


**Fig. 5.** Pareto optimal combinations of thinning ratio and bulge ratio

the forming parameters determined by the approach presented in this study.

### 4.4 Pareto set of this multi-objective optimization problem

As discussed before, if there are many Pareto optimal solutions for a given multi-objective optimization problem, the collection of these Pareto optimal solutions will form the Pareto set of this problem. In this study, the weighting vector is set equal to the goal, a Pareto optimal combination of internal pressure and friction coefficient is obtained and the improvement of the bulge ratio as well as the thinning ratio is confirmed. By varying the values of weights  $w_1, w_2$ , a series of Pareto optimal combinations of internal pressure and friction coefficient can be obtained, these Pareto optimal combinations of internal pressure and friction coefficient will form the Pareto set for the given free bulging tube hydroforming process. In this study, a series of values between 0 and 1 are chosen as the weight  $w_1$ , and the weight  $w_2$  is set equal to one minus  $w_1$ . Based on these different weight vectors, a series of corresponding Pareto optimal solutions are obtained by solving Eq. 14 using the goal attainment method. A series of corresponding bulge ratios and thinning ratios according to the different combination of internal pressure and friction coefficient are obtained by the finite element analyses and plotted in Fig. 5.

The curve in Fig. 5 is the Pareto optimal front of the combination of thinning ratio and bulge ratio for this free bulge hydroforming process. All possible combinations of the thinning ratio and bulge ratio are located on or below the Pareto front. If a specific bulge ratio is required for this process, the obtainable optimal thinning ratio will be the projected point of this bulge ratio from this Pareto optimal front. Conversely, if a given thinning ratio is deemed acceptable, the Pareto optimal front gives the maximum bulge ratio obtainable.

## 5 Conclusions

In this paper, a new method of optimization of the forming parameters for tube hydroforming has been suggested. From the results of the FEM analysis and the effect of parameters study

using the Taguchi method, some useful conclusions can be drawn as follows:

1. The significant forming parameters affecting the hydroformability can be identified easily by performing the experiments designed according to the orthogonal array of the Taguchi method.
2. Internal pressure and the friction coefficient have the greatest effects on a free bulging tube hydroforming process.
3. Eliminating the insignificant parameters for the optimization of the forming parameters results in significant saving of computational time.
4. The bulge ratio and thinning ratio for a given free bulge tube hydroforming process are improved simultaneously through our approach.
5. The corresponding optimal thinning ratio can be obtained according to the Pareto set of the optimization problem if a specific bulge ratio is required for a given free bulge hydroforming process.

---

## References

1. Carleer B, Kevie G, Winter L, Veldhuizen B (2000) Analysis of the effect of material properties on the hydroforming process of tubes. *J Mater Process Technol* 104:158–166
2. Manabe K, Amino M (2002) Effects of process parameters and material properties on deformation process in tube hydroforming. *J Mater Process Technol* 123:285–291
3. Boudeau N, Lejeune A, Gelin JC (2002) Influence of material and process parameters on the development of necking and bursting in flange and tube hydroforming. *J Mater Process Technol* 125–126:849–855
4. Koj M, Altan T (2002) Application of two dimensional (2D) FEA for the tube hydroforming process. *Int J Mach Tool Manuf* 42:1285–1295
5. Yang J, Jeon B, Oh S (2001) Design sensitivity analysis and Optimization of the hydroforming process. *J Mater Process Technol* 113:666–672
6. Park K, Kim Y (1995) The effect of material and process variables on the stamping formability of sheet materials. *J Mater Process Technol* 51:64–78
7. Lee SW (2002) Study on the forming parameters of the metal bellows. *J Mater Process Technol* 130–131:47–53
8. Ko D, Kim D, Kim B (1999) Application of artificial neural network and Taguchi method to preform design in metal forming considering workability. *Int J Mach Tool Manuf* 39:771–785
9. Yang HJ, Hwang PJ, Lee SH (2002) A study on shrinkage compensation of the SLS process by using the Taguchi method. *Int J Mach Tool Manu* 42:1203–1212
10. Duan X, Sheppard T (2002) Influence of forming parameters on the final subgrain size during hot rolling of aluminium alloys. *J Mater Process Technol* 130–131:245–249
11. Yang WH, Tarn YS (1998) Design optimization of cutting parameters for turning operations based on the Taguchi method. *J Mater Process Technol* 84:122–129
12. Huh H, Heo JH, Lee HW (2003) Optimization of a roller levelling process for A17001T9 pipes with finite element analysis and Taguchi method. *Int J Mach Tool Manuf* 43:345–350
13. Anastasiou KS (2002) Optimization of the aluminium die casting process based on the Taguchi method. *Proc Inst Mech Eng B, J Eng Manuf* 216:969–977
14. Dhavlikar MN, Kulkarni MS, Mariappan V (2003) Combined Taguchi and dual response method for optimization of a centerless grinding operation. *J Mater Process Technol* 132:90–94
15. Kim SJ, Kim KS, Jang H (2003) Optimization of manufacturing parameters for a brake lining using Taguchi method. *J Mater Process Technol* 136:202–208
16. Shabeer S, Wang MY (2000) Multi-objective optimization of sequential brakeforming processes. *J Mater Process Technol* 102:266–276
17. Marler RT, Arora JS (2003) Review of Multi-Objective Optimization Concepts and Algorithms for Engineering. Technical Report No. ODL-01.03, Optimal Design Laboratory, The University of Iowa, Iowa City
18. Sauve RG (1999) H3DMAP Version 6 A general three-dimensional linear and nonlinear analysis of structures. Ontario Hydro Technologies Report No. A-NSG-96-120, Revision 1, Toronto
19. Li B, Metzger DR, Nye TJ (2003) Reliability analysis of the tube hydroforming process based on forming limit diagram. *Comput Technol Appl ASME-PVP* 458:301–308
20. Gembicki FW (1974) Vector optimization for control with performance and parameter sensitivity indices. Dissertation, Case Western Reserve University, Cleveland, OH